Spectrochimica Acta Part A 77 (2010) 802–806

Contents lists available at ScienceDirect

Spectrochimica Acta Part A: Molecular and Biomolecular Spectroscopy

journal homepage: www.elsevier.com/locate/saa

Molecular spectroscopic analysis of nano-chitosan blend as biosensor

Medhat Ibrahim[a,b,*], Abdel Aziz Mahmoud[a], Osama Osman[a], Ahmed Refaat[a], El-Sayed M. El-Sayed[c]

[a] Spectroscopy Department, National Research Centre, 12311 Dokki, Cairo, Egypt
[b] Physics Department, Faculty of Science, Jazan University, 2097 Jazan, Saudi Arabia
[c] Physics Department, Biophysics Branch, Faculty of Science, Ain Shams University, 11566 Cairo, Egypt

ARTICLE INFO

Article history:
Received 13 April 2010
Received in revised form 18 July 2010
Accepted 3 August 2010

Keywords:
Chitosan
Starch
Gelatin
FTIR
UV–vis and PM3

ABSTRACT

Chitosan/starch and chitosan/gelatin of different ratios were prepared following casting method. FTIR results indicate the formation of hydrogen bonding which dedicates the prepared blends for interaction with wide range of molecules specially those of NH_2 and COOH terminals. The results obtained with molecular modeling PM3 model are in agreement with spectroscopic data. As a result of increasing starch and gelatin in chitosan blends HOMO–LUMO energy slightly decreased while total dipole moment increased. UV–vis spectroscopy indicated the suitability of chitosan/starch blend as a glycine sensor. Further enhancement in the sensing performance of chitosan/starch blend was achieved by introducing 5 nm TiO_2 into the blend.

1. Introduction

Over the past few decades, the amazing growth in the biomaterial technology has revolutionized their use in biological and industrial fields. Chitosan is widely applied in the biomedical field because it can be obtained from natural sources that are abundant and renewable [1]. Chitosan is easily prepared from chitin, the most abundant compound in nature after cellulose [2]. Chemical modification of chitosan produces materials with a variety of physical and mechanical properties [3–5]. For example, chitosan films and fibers can be formed using cross-linkers and adapted techniques for altering from other polysaccharides, such as treatment of amylose with epichlorohydrin [6]. Like hyaluronic acid, chitosan is not antigenic and is a well-tolerated implanted material [7]. Chitosan can easily be prepared in many forms, including, films and membranes. The basic technique for the casting of chitosan films and fibers was early developed [8,9] by dissolving in a weak organic acid, casting onto a smooth surface, and removal of the anion for the chitosan to exhibit resistance to water [1]. Moreover, gelatin has excellent plasticity, adhesiveness, biocompatibility, and nonantigenicity. It has the potential to mix with chitosan at the suitable pH value due to its ability to form hydrogen bonding. Thus, gelatin was postulated as a suitable candidate to be blended with chitosan [10]. Although chitosan films are highly impermeable to oxygen, they have relatively low water vapor barrier characteristics. In order to prepare membranes with modified water vapor barrier, starch was blended with chitosan [11]. Starch was used to produce biodegradable films to be used in various applications because of its low cost and renewability. However, wide application of starch film is limited by its water solubility and brittleness [12]. Recently chitosan blends continue to be a topic of much research work [13–15].

The present work was conducted to prepare chitosan blends in which a cross-linker could improve the surface properties of chitosan. Accordingly, chitosan was prepared using casting method with gelatin and starch. The molecular structure of the prepared films was studied with FTIR. In addition, semiemperical quantum mechanical PM3 method was used to calculate ionization potential, HOMO-LUMO energy, and the total dipole moment for chitosan as well as the studied chitosan blends. The prepared blend was used as a biosensor for the amino acid glycine.

2. Materials and methods

2.1. Reagents

Chitosan low molecular weight was purchased from ABCO Laboratories Eng. Ltd (Gillingham, England).

Soluble starch, extra pure AR, was obtained from Sissco Research Laboratories Pvt. Ltd (Bombay, India).

Gelatin from bovine skin, Type B obtained from Sigma–Aldrich (Steinheim, Germany).

Glycine was purchased from Adwic Company (Cairo, Egypt).

* Corresponding author at: Spectroscopy Department, National Research Centre, 12311 Dokki, Cairo, Egypt. Tel.: +20 122727636; fax: +20 233370931.
E-mail addresses: medahmed6@yahoo.com, methat.ibrahim@gmail.com (M. Ibrahim).

1386-1425/$ – see front matter © 2010 Elsevier B.V. All rights reserved.
doi:10.1016/j.saa.2010.08.007

Table 1
Prepared blend films contents in mg.

Chitosan, mg	Polymer content, mg		Blend ratio, %
	Starch	Gelatin	
100	0	0	0.00
90	10	0	10.00
90	0	10	10.00
80	20	0	20.00
80	0	20	20.00
50	50	0	50.00
50	0	50	50.00
30	70	0	70.00
30	0	70	70.00

2.2. Polymer blend preparations

Chitosan was mixed with different polymers namely, starch and gelatin to get several blends in the form of films. The mixing ratios were followed as indicated in Table 1. The mixtures containing chitosan starch and chitosan gelatin were added to 100 ml acetic acid (7% solution) at room temperature with stirring until a homogeneous solution was obtained. The solution was distributed into leveled hydrophobic polystyrene Petri dishes (10 cm diameter). To get the desired films, the solution was left to dry for 48 h at room temperature in open air. Complete drying was avoided since some moisture is required for films to remain flexible. Films were finally peeled off from the trays and placed in sealed containers to avoid moisture exchange [8].

2.3. Sensing experiment

1 M glycine solution was prepared and then diluted into 10^{-1}, 10^{-2}, 10^{-5}, and 10^{-6} M respectively.

The TiO_2 was prepared by precipitation method [16] using titanium tetrachloride ($TiCl_4$) as a precursor and the grain size of the obtained TiO_2 was about 5 nm as estimated by STEM (Fig. 1). The prepared TiO_2 was then added to the chitosan/starch blend for sensing experiment.

In order to test the blend films as biosensors for glycine, the films were cut into 0.5 cm × 3 cm strips then inserted into different glycine solutions for 30 s up to 5 min.

2.4. Instrumentations

Fourier Transform Infrared Spectroscopy (*FTIR*): Jasco FTIR 430 Fourier Transform Infrared Spectrometer was used for recording the obtained IR spectra. Spectra were recorded in a spectral range of 4000–400 cm^{-1}, resolution of 4 cm^{-1} and scan speed is 2 mm/s.

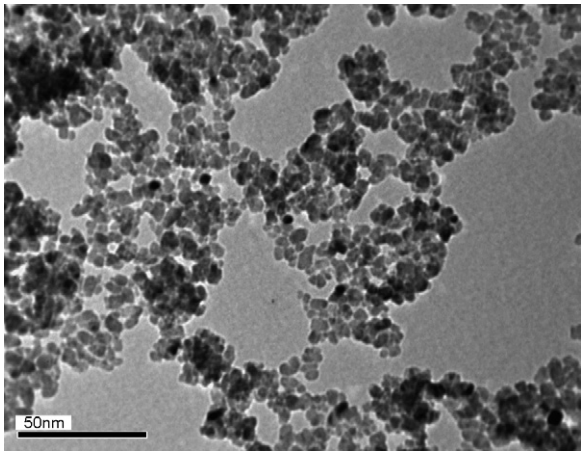

Fig. 1. STEM of the prepared TiO_2; the estimated grain size is 5 nm.

UV/Vis/NIR Spectrometer: Jasco-V.570 UV/Vis/NIR Spectrophotometer was used for recording the UV spectra. Spectra were recorded in a spectral range of 700–190 cm^{-1}.

2.5. Calculation details

Fig. 2 shows a model molecule of 10 chitosan units is built. The amino acid alanine is used as a model molecule for gelatin.

For chitosan/starch and chitosan/gelatin blends 1, 2, 5 and 7 units (starch and/or gelatin) were replaced instead of chitosan to form blends with ratios 10%, 20%, 50 and 70%, respectively. Glycine interacted as a weak interaction with the hydrogen bonding of NH_2 to test the chitosan/starch blend as a biosensor. All the model molecules were studied using MOPAC 2002, as implemented in the CAChe program [17] at PM3 level of theory. First the geometry is optimized then the ionization potential, HOMO/LUMO energy and the total dipole moment are calculated at the same level of theory.

3. Results and discussion

3.1. FTIR results of pure polymer

FTIR is a very useful tool for detecting interactions in polymer blends. FTIR was, therefore, applied to examine the possible interactions between the blend components.

The FTIR absorption spectrum of chitosan is shown in Fig. 3. The broad band at 3409 cm^{-1} was due to the OH stretching vibration. The band at 2921 cm^{-1} was due to the CH stretching. The band at 1954 cm^{-1} is the characteristic absorption band of NH_2. The band at 1657 was due to the OH of chitosan [18]. The band at 1519 cm^{-1} is due to the scanty amount of O=C–NH_2. Bands around 1422 and 1383 cm^{-1} are assigned to the CH_2 and CH_3 vibrations respectively. The region from 1152 to 1033 cm^{-1} is the characteristic band of C–O–C linkage. Finally, the C–N fingerprint band appears at 896 cm^{-1}.

The structure of starch is similar to chitosan which in turn leads to similar FTIR characteristics. Chitosan has an amino group on the C2 carbon rather than a hydroxyl group of starch. The band assignments of starch are also shown in Fig. 3. The broad band at 3408 cm^{-1} was due to the stretching mode of the OH groups. An intense band at 1654 cm^{-1} was assigned to the first overtone of the OH bending vibration. The bands at 1154 and 2929 cm^{-1} were assigned to C–O stretching and CH stretching, respectively [18]. Two strong bands at 1082 and 1006 cm^{-1} were attributed to CH_2–O–CH_2 stretching vibrations [18].

The absorption band at 3299 cm^{-1} arises from NH stretching, the one at 1638 cm^{-1} is attributed to amide I, C=O and CN stretching, that at 1545.51 cm^{-1} is assigned as amide II and 1243 cm^{-1} is amide III [19]. The last bands can be assigned to the characteristic bands of gelatin. The band at 2923 cm^{-1} represents the CH_2 asymmetric stretching vibration that is followed by another band at 2850 cm^{-1} which is corresponding to symmetric stretching vibration of CH_2 [20]. The CH_2 bending and wagging vibrations give raise to two bands at 1452 and 1337 cm^{-1} respectively. Finally the skeletal stretching arises at both 1081 and 668 cm^{-1}, respectively [20].

3.2. FTIR results of the studied blends

When two or more substances (such as biopolymers) are mixed, physical blends versus chemical interactions are reflected by noticeable changes in characteristic bands [21,22]. Accordingly; blending two polymers is an approach to develop new biomaterials

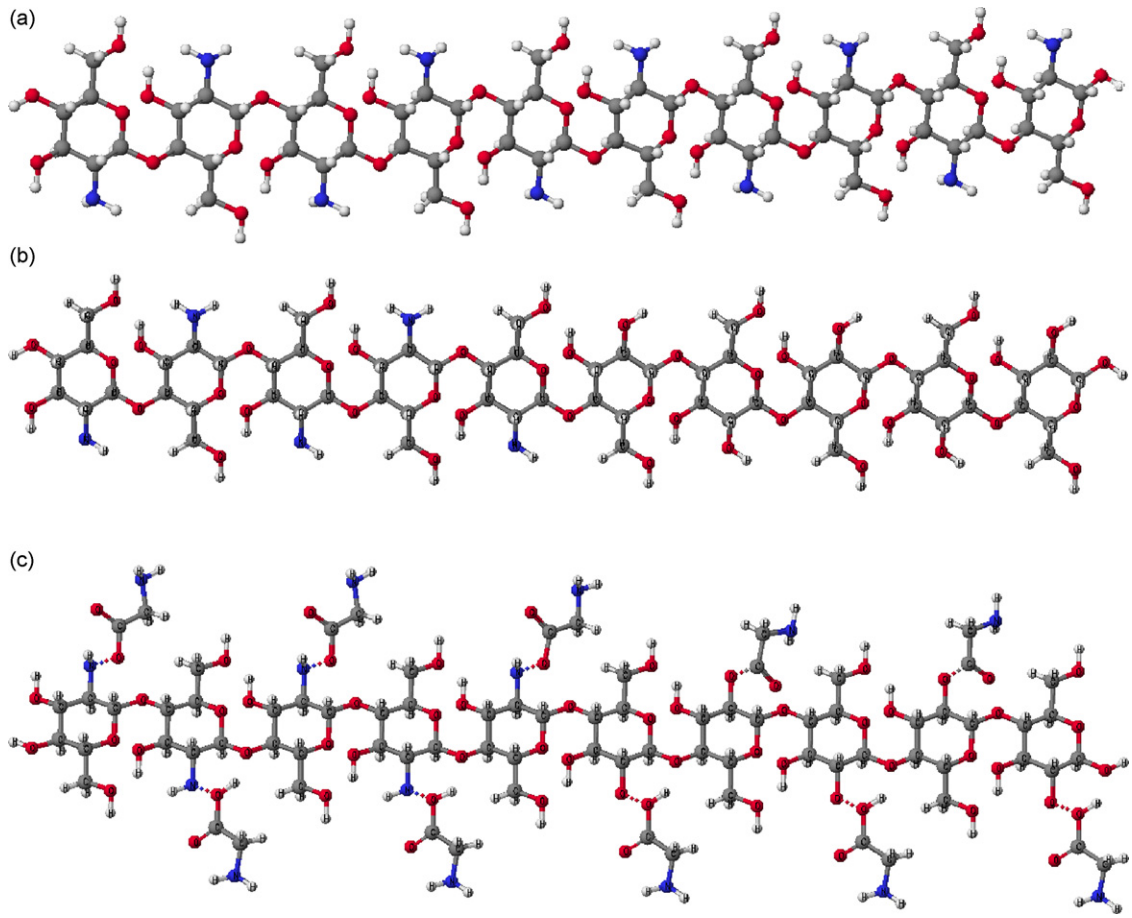

Fig. 2. (a) Model molecule of chitosan which consists of 10 units. In the studied blends, starch and gelatin are interacted with chitosan through O-linkage f chitosan. (b) Model molecule of chitosan/starch blend which consists of 10 units. 5 units of chitosan are linked with 5 starch units through O-linkage. (c) Model molecule of chitosan/starch blend whereas glycine is interacted as a weak interaction through the NH_2 of chitosan and OH of starch.

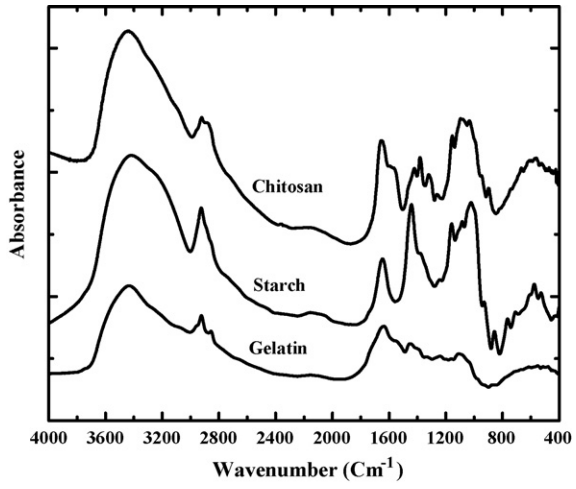

Fig. 3. FTIR absorption spectra for chitosan, starch and gelatin respectively.

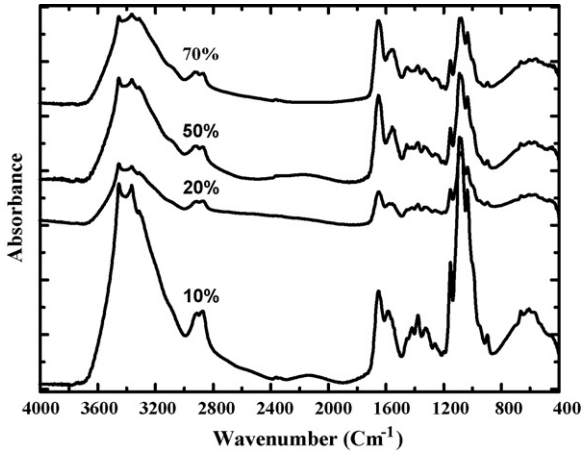

Fig. 4. FTIR absorption spectra for chitosan/gelatin blends.

exhibiting combinations of properties that could not be obtained by individual polymers [23]. The analysis of FTIR spectrum of each blend enables studying the interactions which possibly take place.

3.2.1. Chitosan/gelatin

The FTIR spectra of the chitosan/gelatin composite films are shown in Fig. 4. The FTIR spectrum of chitosan film displayed bands around 901 and 1155 cm^{-1}, are assigned to the saccharine structure and an amino characteristic band at 1519 cm^{-1}. There was a stronger absorption band at 1633 cm^{-1} corresponding to the amide of chitosan. Gelatin film was characterized by its amino band at 1545 cm^{-1} and carbonyl band at 1638 cm^{-1}. Incorporation of gelatin led to small shifts in the positions of amide I and amide II of chitosan toward the higher frequencies. These findings were attributed to the formation of amide and tertiary amine linkages between chitosan and gelatin macromolecules [24].

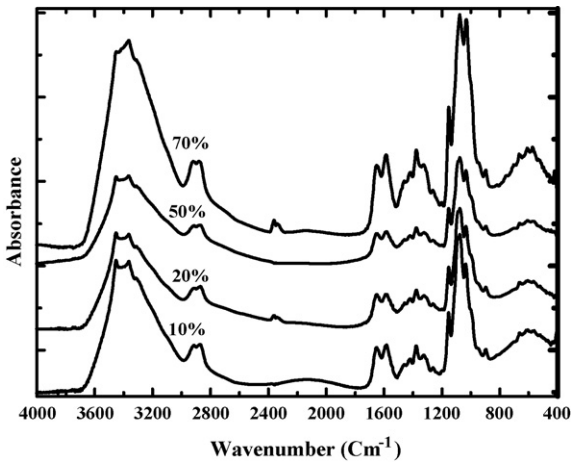

Fig. 5. FTIR absorption spectra for chitosan/starch blends.

3.2.2. Chitosan/starch

Fig. 5 reflects the typical spectra of chitosan/starch blend films. As mentioned earlier; the FTIR spectra of the, starch consists of three characteristic bands between 1006 and 1154 cm^{-1}, which are attributed to the C–O bond stretching [18]. The band at 1654 cm^{-1} is assigned to the OH bending of water [18]. The band at 1467 cm^{-1} is assigned to the CH2 bending. The sharp band at 2929 cm^{-1} is the characteristic of CH stretches associated with the ring methane hydrogen atoms. An extremely broad band occurs at 3408 cm^{-1} due to the hydrogen-bonded hydroxyl groups that contribute to the complex vibrational stretches associated with free inter- and intramolecular bound hydroxyl group, which make up the gross structure of starch [25]. In chitosan, the band at 2921 cm^{-1} is typical of CH stretching vibration [18]. The band at 1739 cm^{-1} suggested the presence of carbonyl group. The one at 1633 cm^{-1} was due to the C=O stretching (amide I). The sharp band at 1377 cm^{-1} corresponds to the CH3 vibration. The broad band at 1076 cm^{-1} indicates the C–O stretching vibration in chitosan. When two or more substances are mixed, physical blends versus chemical interactions are reflected by changes in characteristic spectral bands. In the typical spectrum of chitosan/starch blend film, the amino band of chitosan shifted from 1519 to 1583 cm^{-1} with the addition of starch. This result indicated that interactions were present between the hydroxyl groups of starch and the amino groups of chitosan [26]. The obtained FTIR spectrum of chitosan/starch blend suggested that the two forming blend were compatible and an interaction existed between them.

3.3. Molecular modeling of chitosan blends

Three important physical parameters were calculated at PM3 semiemperical method namely total dipole moment; ionization potential and HOMO–LUMO energy. Table 2 presents the calculated PM3 parameters. The calculated parameters will be discussed in comparison with those of chitosan. The results revealed slight increase in ionization potential with increasing starch content, while slightly decreases HOMO–LUMO energies. Although total dipole moment has decreased corresponding to starch 10% and 20%; a noticeable increase happens as starch content increased up to 70%.

Table 2
Calculated ionization potential (IP) as eV; HOMO–LUMO energy (ΔE) as eV and total dipole moment (TDM) as debye for the studied blends.

Blend	IP	ΔE	TDM
Chitosan	9.980	10.917	6.092
Chitosan/starch (10%)	9.582	10.958	4.340
Chitosan/starch (20%)	9.621	10.961	4.887
Chitosan/starch (50%)	9.692	10.733	9.311
Chitosan/starch (70%)	9.738	10.175	11.861
Chitosan/gelatin (10%)	8.346	7.980	4.699
Chitosan/gelatin (20%)	9.281	9.681	3.462
Chitosan/gelatin (50%)	8.945	7.347	10.837
Chitosan/gelatin (70%)	8.654	10.739	16.169

Table 3
Calculated ionization potential (IP) as eV; HOMO–LUMO energy (ΔE) as eV and total dipole moment (TDM) as debye for the possible interaction between glycine and chitosan/starch (5:5) blend.

Blend	IP	ΔE	TDM
Chitosan/starch (50%)	9.692	10.733	9.311
Chitosan/starch/glycine (50%)	8.137	9.053	17.614

Regarding chitosan/gelatin blend the calculated ionization potential has decreased as compared with that of chitosan pure. The same happens for the calculated HOMO–LUMO energy. Finally the calculated total dipole moment increases as the gelatin content increased. Correlating these results with our previous findings [27,28] has revealed that the increase in total dipole moment reflects the increasing of interaction abilities of a given structure. As a result of blend formation the ability of interaction increased in terms of the calculated dipole moment. This result is supported with the slight decrease in ionization potential and HOMO–LUMO energy.

As an application example, one of the studied blends was chosen for possible interaction with the amino acid glycine. The chitosan/starch (50%) was chosen. Glycine was supposed to interact with the blend surface as a weak hydrogen bonding. The H-bonding of COOH (amide) is supposed to interact with H-bonding of NH_2 of chitosan also with the H-bonding of OH group of starch. The proposed structure of this interaction is indicated in Fig. 1c. At the same level of theory the ionization potential, HOMO–LUMO energy and total dipole moment are calculated. Regarding Table 3 one can notice that, the calculated ionization potential has taken as glycine interacted with the blend from 9.692 to 8.137 eV. The calculated energy band gap also decreased from 10.733 to 9.053 eV, while the total dipole moment increased from 9.311 to 17.614 debye. This indicates that the surface of a given blend has become more reactive for the interaction. Even the interaction became much better as a result of hydrogen bonding formation with structures containing amide group. The calculated parameters indicate also that the prepared blends could be used as sensors for protein. This result paves the way toward surface modification of these blends to be applied widely in the field of biosensors.

3.4. Chitosan nano-blend as biosensor

UV–vis spectroscopy is used to elucidate the efficiency of the prepared blends as sensor for glycine. As seen in Table 4 the absorbance of 10^{-1}, 10^{-2}, 10^{-5}, and 10^{-6} M glycine solutions were recorded. Then films of chitosan; chitosan/starch and chitosan/starch/TiO_2 were inserted separately into the glycine of the same concentrations. The time of insertion was ranging from

Table 4
Glycine absorbance as obtained on the UV/vis spectrophotometer both before and after applying the film stripes.

	Glycine concentration			
	10^{-1} M	10^{-2} M	10^{-5} M	10^{-6} M
Std glycine	1.6811	1.2883	1.0927	0.9949
Cs	1.6318	1.2692	1.0775	0.8675
Cs/Str	1.2650	0.5783	0.1739	0.2248
Cs/Str/TiO_2	1.1713	0.4945	0.0602	0.0723

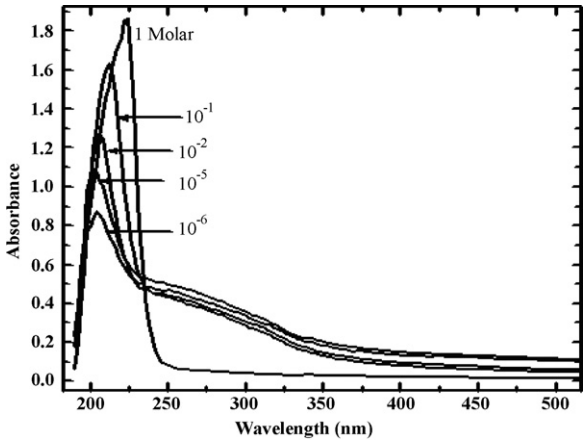

Fig. 6. UV–vis absorption spectra for the glycine after exposed to chitosan film at different concentrations from 1 mol up to 10^{-6} mol. The shift in the absorption band toward higher wavelengths is attributed to the increase in the pH values [29].

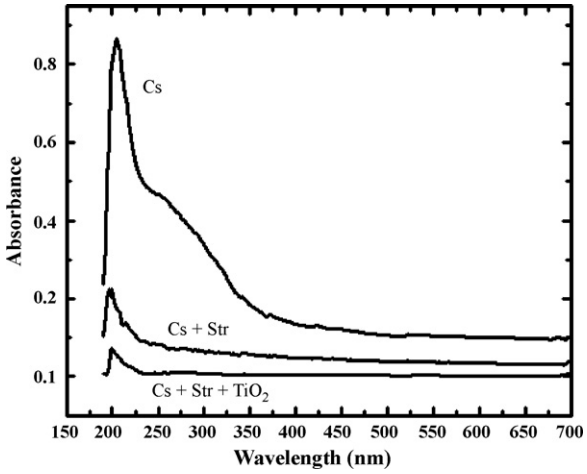

Fig. 7. UV–vis spectra of glycine amino acid (10^{-6} M) as exposed to chitosan (Cs), chitosan/starch blend (Cs + Str) and nano-chitosan/starch/TiO_2 blend.

30 s up to 5 min. No change in absorbance were recorded accordingly the results in Table 4 and Figs. 6 and 7 are taken to represent the insertion time 30 s.

Fig. 6 shows that as chitosan films are inserted into glycine solution a decrease in absorbance took place. This is attributed to the physical interaction between glycine and chitosan through the formation of hydrogen bonding between the carboxylic group (COO^-) of glycine and the amino group (NH_2) of chitosan. As the concentration of the glycine increased a shift in the characteristic band is shifted toward higher wavelengths. It is stated that, the shift in the absorption band toward higher wavelengths is attributed to the increase in the pH values [29].

Fig. 7 indicates that as chitosan/starch blend inserted into glycine solution the films show better sensitivity as compared with pure chitosan. Further enhancement in the sensing property of the blend was achieved by the help of TiO_2, the estimated grain size of which is 5 nm. It was found that after the addition of TiO_2 to the films, glycine absorbance decreased sharply by approximately 65% up to 75%. Accordingly the surface enhancement of the blend surface provides better opportunities for the formation of hydrogen bonding and accordingly enhancing the application of such nano-blend as a biosensor.

4. Conclusion

The obtained PM3 model indicates an increase in total dipole moment of chitosan blends with slight decrease in both ionization potential and HOMO–LUMO energy. These proposed the ability of chitosan blends to interact with surrounding molecules. FTIR indicates the existence of hydrogen bonding and dedicate the prepared films for detecting structures containing NH_2 and COOH. UV spectroscopy indicates the suitability of chitosan/starch for detecting glycine. Further enhancement in blend sensitivity is achieved as nano-TiO_2 introduced into the chitosan/starch blend. Accordingly nano-chitosan/starch/TiO_2 blend could be utilized as biosensor.

References

[1] M. Sakkinen, Biopharmaceutical evaluation of crocrystalline chitosan as release-rate-controlling hydrophilic polymer in granules for gastro-retentive drug delivery, Academic Dissertation, Division of Biopharmaceutics and Pharmacokinetics, Department of Pharmacy, University of Helsinki, Finland, 2003.
[2] G.A.F. Roberts, Chitin Chemistry, The Mac Millan Press, London, 1992, pp. 1–110 and 274–315.
[3] R. Muzzarelli, V. Baldassara, E. Conti, P. Ferrara, G. Biagini, G. Gazzarelli, V. Vasi, Biomaterials 9 (1988) 247–252.
[4] E. Wang, S.E. Overgaard, J.M. Scharer, N.C. Bols, M. Moo-Young, Chitosan, Biotechnol. Tech. 2 (1988) 133–136.
[5] M. Laleg, I. Pikulik, Nord. Pulp Paper Res. J. 9 (1991) 99–103.
[6] J.C. Wei, S.M. Hudson, J.M. Mayer, D.L. Kaplan, J. Polym. Sci. 30 (1977) 2187–2193.
[7] W. Malette, M. Quigley, E. Adicks, Chitosan effect in vascular surgery, tissue culture and tissue regeneration, in: R. Muzzarelli, C. Jeuniaux, G. Gooday (Eds.), Chitin in Nature and Technology, Plenum, New York, 1986, pp. 435–442.
[8] G. Rigby, Process for the preparation of films and filaments and products thereof, USA Patent No. 2,030,880 (19 May 1936).
[9] G. Rigby, Substantially undegraded deacetylated chitin and processes for producing the same, USA Patent No. 2,040,879 (19 May 1936).
[10] M. Cheng, J. Deng, F. Yang, Y. Gong, N. Zhao, X. Zhang, Biomaterials 24 (2003) 2871–2880.
[11] Y.X. Xu, K.M. Ki, M.A. Hanna, D. Nag, Indus. Crops Prod. 21 (2004) 185–192.
[12] Q.X. Wu, L.N. Zhang, J. Appl. Polym. Sci. 79 (2001) 2006–2013.
[13] S. Ludwiczak, M. Mucha, Carbohydr. Polym. 79 (2010) 34–39.
[14] V.N. Malheiro, S.G. Caridade, N.M. Alves, J.F. Mano, Acta Biomater. 6 (2010) 418–428.
[15] J. Li, S. Zivanovic, P.M. Davidson, K. Kit, Carbohydr. Polym. 79 (2010) 786–791.
[16] W. Zhang, S. Chen, S. Yu, Y. Yin, J. Cryst. Growth 308 (2007) 122–129.
[17] J.J.P Stewart, MOPAC 2002 Version 2.5.3, Fujitsu Limited, Tokyo, Japan, 2002.
[18] L. You, F. Lu, D. Li, Z. Qiao, Y. Yin, J. Hazard. Mater. 172 (2009) 38–45.
[19] R. Yin, Y. Huang, C. Huang, Y. Tong, N. Tian, Mater. Lett. 63 (2009) 1335–1337.
[20] J.H. Muyonga, C.G.B. Cole, K.G. Duodu, Food Chem. 86 (2004) 325–332.
[21] Y.L. Guanet, X.F. Liu, Y.P. Zhang, K.D. Yao, J. Appl. Polym. Sci. 67 (1998) 1965–1972.
[22] Y.Y. Cheng, J.B. Ma, Polym. Int. 48 (1999) 429–433.
[23] M. Ratajska, S. Boryniec, React. Funct. Polym. 38 (1998) 35–40.
[24] V. Chiono, E. Pulieri, G. Vozzi, G. Ciardelli, A. Ahluwalia, P. Giusti, J. Mater. Sci.: Mater. Med. 19 (2008) 889–898.
[25] J.M. Fang, P.A. Fowler, J. Tomkinso, C.A.S. Hill, Carbohydr. Polym. 47 (2002) 245–252.
[26] F. Liu, B. Qin, L. He, R. Song, Carbohydr. Polym. 78 (2009) 146–150.
[27] M. Ibrahim, H. El-Haes, Int. J. Environ. Pollut. 23 (2005) 417–424.
[28] M. Ibrahim, M. Mahmoud, J. Comput. Theor. Nanosci. 6 (2009) 1523–1526.
[29] J.S. McConnel, R.M. McConnel, L. Hossner, Ultraviolet spectra of acetic acid, glycine and glyphosate, Proceed. Arkansas Acad. Sci. 47 (1993) 73–76.